Clim. Past Discuss., 11, 221–241, 2015
www.clim-past-discuss.net/11/221/2015/
doi:10.5194/cpd-11-221-2015

Climate of the Past
Discussions
Open Access

Obliquity forcing of low-latitude climate

J. H. C. Bosmans[1,2,*], **F. J. Hilgen**[1], **E. Tuenter**[2,1,**], **and L. J. Lourens**[1]

[1]Faculty of Geosciences, Utrecht University, the Netherlands
[2]Royal Netherlands Meteorological Institute (KNMI), the Netherlands
[*]now at: Utrecht University
[**]now at: KNMI

Received: 16 January 2015 – Accepted: 27 January 2015 – Published: 11 February 2015

Correspondence to: J. H. C. Bosmans (j.h.c.bosmans@uu.nl)

Published by Copernicus Publications on behalf of the European Geosciences Union.

Abstract

The influence of obliquity, the tilt of the Earth's rotational axis, on incoming solar radiation at low latitudes is small, yet many tropical and subtropical paleoclimate records reveal a clear obliquity signal. Several mechanisms have been proposed to explain this signal, such as the remote influence of high-latitude glacials, the remote effect of insolation changes at mid- to high latitudes independent of glacial cyclicity, shifts in the latitudinal extent of the tropics, and changes in latitudinal insolation gradients. Using a sophisticated coupled ocean–atmosphere global climate model, EC-Earth, without dynamical ice sheets, we performed two experiments of obliquity extremes. Our results show that obliquity-induced changes in tropical climate can occur without high-latitude ice sheet fluctuations. Furthermore, the tropical circulation changes are consistent with obliquity-induced changes in the cross-equatorial insolation gradient, implying that this gradient may be used to explain obliquity signals in low-latitude paleoclimate records instead of the classic 65° N summer insolation curve.

1 Introduction

The influence of obliquity (axial tilt) on low-latitude insolation is very small; the difference over tropical latitudes between high and low obliquity is less than $10\,\mathrm{W\,m^{-2}}$ in the summer or winter season, whereas precession-induced insolation changes reach $100\,\mathrm{W\,m^{-2}}$ (Tuenter et al., 2003; Bosmans et al., 2014a). A power spectrum of insolation at the tropics (23° N, roughly the Tropic of Cancer) shows a peak at the periodicity of precession (~ 23 kyr), but not obliquity (~ 41 kyr), whereas insolation at 65° N shows a much larger influence of obliquity (Fig. 6). The 65° N insolation curve also correlates better with low-latitude paleoclimate records, such as the Mediterranean sapropels, than low-latitude insolation (e.g. Lourens et al., 1996; Lourens and Reichart, 1996). Many studies have therefore attributed the relatively strong obliquity signal in low-latitude paleoclimate records to high-latitude mechanisms. For instance, dust flux records from both the (sub-)tropical Atlantic and Arabian Sea concur with obliquity-paced global climate cycles, suggesting a close link between changes in low-latitude aridity and glacial variability (Bloemendal and deMenocal, 1989; deMenocal et al., 1993; deMenocal, 1995; Tiedemann et al., 1994). Several other proxy studies, however, find low-latitude obliquity signals at times when glacial cycles were much smaller or even absent (Lourens et al., 1996, 2001; Hilgen et al., 1995, 2000; Sierro et al., 2000). In particular, obliquity-controlled interference patterns in Mediterranean sapropels are not only present in the Pleistocene (Lourens et al., 1996), but also in the warmer Pliocene and Miocene (Hilgen et al., 1995). Sapropels are generally thought to be related to African monsoon strength through runoff from African rivers into the Mediterranean (Rossignol-Strick, 1985), which would indicate that monsoon intensity is affected by obliquity both before and after major Northern Hemisphere (NH) glacial cycles determined global climate. Furthermore, in the late Pliocene and Pleistocene, phase relations suggest that the obliquity influence on sapropel formation and North-African aridity did not proceed indirectly via ice driven responses but more directly via summer insolation (Lourens et al., 1996, 2010). In addition, color changes associated with carbonate dilution cycles in north-western Africa and Spain reveal precession-obliquity interference patterns similar to those found in Mediterranean sapropels (Hilgen et al., 2000; Sierro et al., 2000). Also, others have ruled out global ice volume as a primary forcing mechanism for the occurrence of obliquity-related variability in Indian monsoon strength as inferred from sediment records of the Arabian Sea (Clemens et al., 1991; Clemens and Prell, 2003).

Hence the North-African and Indian monsoons may respond to obliquity independent of high-latitude ice growth and decay. The driving mechanism of obliquity-induced climate change over the tropics is yet poorly understood, since the influence of obliquity on low-latitude insolation is small. Some studies have suggested that the obliquity signal in the tropics is related to a local forcing mechanism. Rossignol-Strick (1985) introduced a monsoon index based on the summer insolation difference between the tropic of Cancer and the equator, recognising that the North-African monsoon depends

CPD
11, 221–241, 2015

on the strength of the Saharan heat trough as well as on the pressure gradient between the heat trough and the equator. The summer insolation difference between these two latitudes introduces an obliquity signal, though too small to explain the characteristic obliquity interference patterns in the Mediterranean sapropels. Lourens and Reichart (1996) therefore introduced the Summer Inter Tropical Insolation Gradient (SITIG), $I_{23^\circ\,N}$–$I_{23^\circ\,S}$ at 21 June (Fig. 6), which shows a better fit to the sapropel record. This gradient is based on the interhemispheric pressure gradient between the two limbs of the winter hemisphere Hadley cell, which drives monsoon winds into the summer hemisphere. At times of high obliquity, the insolation gradient over the tropics (SITIG) is stronger than during low obliquity. This also holds for SITIG in austral summer, $I_{23^\circ\,S}$–$I_{23^\circ\,N}$ at 21 December. A strong SITIG may result in stronger cross-equatorial winds and moisture transport into the summer hemisphere, associated with an intensified winter Hadley cell (Lourens and Reichart, 1996). SITIG can therefore explain the obliquity signal in the sapropels (through monsoonal runoff) as well as the Indian ocean proxy records without high-latitude mechanisms. We note that obliquity may also affect climate through other insolation gradients (e.g. Lourens and Reichart, 1996; Leuschner and Sirocko, 2003; Raymo and Nisancioglu, 2003; Antico et al., 2010; Mantsis, 2011), which will be considered in the Discussion (Sect. 4).

Modelling results previously suggested that the influence of obliquity on the tropics resulted from high latitude forcing, i.e. consistent with the application of the 65° N insolation curve. According to Tuenter et al. (2003), an increase in obliquity results in higher temperature and humidity at high latitudes. The resulting strengthening of southward moisture transport as well as a stronger Asian low pressure system act to strengthen the monsoons. This remote control (north of 30° N) accounts for 80–90 % of the total obliquity signal in the North-African monsoon, without any changes in land ice (Tuenter et al., 2003). The model they used is EC-Bilt (Opsteegh et al., 1998), a quasi-geostrophic climate model of intermediate complexity. Due to simplifications in model physics as well as low resolution one can question its suitability for modeling tropical climate. Bosmans et al. (2014a) showed, using a state-of-the-art high resolution fully

CPD
11, 221–241, 2015

J. H. C. Bosmans et al.

coupled ocean–atmosphere model, EC-Earth, that mechanisms behind the orbital forcing of the North-African monsoon are very different than previously established from the EC-Bilt model. From EC-Earth it emerged that while the effect of precession was larger, a clear obliquity signal appeared in the monsoon as well without high-latitude influences.

In this study we the EC-Earth model to investigate the influence of obliquity signal on the entire tropics (without land ice changes). Specifically, we investigate whether our results are in line with the SITIG mechanism. The model and experimental set-up are described in Sect. 2. The results in Sect. 3 describe changes in atmospheric circulation that can help explain paleoclimate records, which usually reflect changes in precipitation (for example dust records or the sapropels) and/or wind (such as Arabian Sea records). The results are followed a discussion in Sect. 4 and a conclusion in Sect. 5. Figures of model results show the difference between high and low obliquity.

2 Model and experimental set-up

Here we use the new, state-of-the-art high resolution fully coupled ocean–atmosphere model, EC-Earth, to investigate influence of obliquity signal on the tropics. EC-Earth is used for the Fifth Assessment Report of the Intergovernmental Panel on Climate Change (Hazeleger et al., 2011) and was also used to perform the pre-industrial and Mid-Holocene experiments of the Paleoclimate Modelling Intercomparison Project (Bosmans et al., 2012). Following Tuenter et al. (2003), we performed two obliquity experiments, one with a low obliquity (22.04°, Tmin) and one with a high obliquity (24.45°, Tmax). Eccentricity is set to zero, so the Earths orbit is perfectly round and there is no influence of precession. All other boundary conditions are fixed at pre-industrial levels, therefore there are no changes in land ice or in vegetation. The experiments were run for 100 years each, which is sufficient for atmospheric and surface variables, including sea surface temperature, to equilibrate to the insolation forcing. For more details see

CPD
11, 221–241, 2015

Title Page
Abstract Introduction
Conclusions References
Tables Figures
◂ ▸
Back Close
Full Screen / Esc
Printer-friendly Version
Interactive Discussion

Bosmans et al. (2014a), where the same obliquity experiments are used to investigate the North African monsoon.

3 Results

EC-Earth shows significant differences in net precipitation over the tropics between high (Tmax) and low obliquity (Tmin, Fig. 1). There is an overall intensification of the North African and Asian monsoons during boreal summer (June-July-August), with a redistribution of precipitation from ocean to land and stronger landward monsoon winds (Fig. 1a, Bosmans et al., 2014a). Over the equatorial and southern Pacific wind speed changes are small while winds around the North Pacific as well as the North Atlantic Highs are generally stronger. During austral summer (December-January-February) net precipitation and wind changes are smaller than during boreal summer, likely related to the smaller land mass and therefore weaker monsoons on the Southern Hemisphere (SH). The largest net precipitation increases occur over the South American and South African summer monsoon regions as well as the Atlantic and Indian Ocean, while net precipitation over the NH tropics is reduced (Fig. 1b).

Our experiments indicate, in agreement with the SITIG mechanism, strengthened surface winds towards the summer hemisphere during Tmax (Fig. 1a and b). The zonal mean cross-equatorial surface winds are northward and they are indeed stronger during boreal summer, extending slightly further into the NH (Fig. 2a). With these stronger surface winds the moisture transport into the NH is strengthened as well during Tmax (Fig. 2b). Moisture transport into the North-African and Asian monsoon areas is generally higher during boreal summer, with enhanced northward cross-equatorial transport mostly over the Indian Ocean (see Fig. 4a). Changes over the Pacific are small, which could be related to the absence of land masses which have a stronger response to insolation changes.

During austral summer the zonal mean southward cross-equatorial surface winds are stronger when obliquity is high (Tmax), extending slightly further into the SH (Fig. 2c).

CPD
11, 221–241, 2015

Obliquity forcing of low-latitude climate

J. H. C. Bosmans et al.

Therefore more moisture is transported southward across the tropics (Fig. 2d). Most of this increased southward moisture transport occurs over the Indian Ocean (Fig. 4b), where both wind and specific humidity are increased. Over the tropical Atlantic specific humidity is lower during Tmax, so moisture transport is not increased despite the increase in wind speed (Fig. 1b).

The changes in surface winds and moisture transport can be related to changes in the (winter) Hadley cell. During boreal summer, the descending branch, centered at $\sim 20^\circ$ S, is strengthened, mostly at the northern side, with a slight weakening at the southern side during Tmax (Fig. 5a). The same holds for the ascending branch, centered at $\sim 10^\circ$ N, so the winter Hadley cell is slightly stronger and extends further into the NH during boreal summer. During austral summer, the winter Hadley cell extends from a descending branch at $\sim 20^\circ$ N to an ascending branch at $\sim 10^\circ$ S (Fig. 5b). The additional rising branch at 5–10° N is most likely overestimated in the model due to a double-ITCZ over the Pacific, a feature that many models encounter (Lin, 2007). However, a strengthening of the winter Hadley cell can still be seen: both the descending and ascending branches are slightly stronger and extend further south during Tmax, in line with stronger southward surface winds.

While winds and moisture transport in the tropics are generally stronger during boreal and austral summer, they are weaker in the annual mean for Tmax (Figs. 1c, 2e and f, 4c). This weakening can be related to the obliquity-induced redistribution of annual mean insolation from low to high latitudes during Tmax, resulting in weakening of the equator-to-pole insolation gradient. Therefore annual mean meridional winds and moisture transport as well as the annual mean Hadley circulation are weaker (Fig. 5c). Annual mean precipitation changes resemble mostly the JJA changes over the continents, and reflect both JJA and DJF changes over the oceans (Fig. 1c).

CPD
11, 221–241, 2015

4 Discussion

We have shown that changes in low-latitude climate can arise as a direct result of obliquity-induced insolation changes, using the sophisticated model EC-Earth. Here we discuss that these changes support the previously proposed SITIG theory (Lourens and Reichart, 1996; Leuschner and Sirocko, 2003), what the implications are for the interpretation of obliquity signals in low-latitude paleoclimate records and how obliquity-induced gradients may influence global climate.

4.1 Model support for the SITIG theory

The simulated changes in winter Hadley cell strength during boreal and austral summer are in accordance with the SITIG theory (Lourens and Reichart, 1996; Leuschner and Sirocko, 2003). The Summer Inter Tropical Insolation Gradient (SITIG, $I_{23^\circ\,N}$–$I_{23^\circ\,S}$ at 21 June) theory states that an increased SITIG during high obliquity (Tmax) is associated with an intensified winter Hadley cell and stronger cross-equatorial winds and moisture into the summer hemisphere. The winter Hadley cell is not entirely symmetric about the equator (as is assumed in the original SITIG hypothesis, Lourens and Reichart, 1996), nor are the changes in wind and moisture transport zonally invariant, likely due to differences in the land-sea distribution. Nonetheless, a stronger SITIG during high obliquity (Tmax) results in stronger zonal mean winds and moisture transport into the summer hemisphere and a stronger Hadley cell in our EC-Earth results. The Hadley cell as well as the meridional winds and moisture transport also extend farther into the summer hemisphere. This is in agreement with the poleward shift of the latitude of the tropics during Tmax (Rossignol-Strick, 1985; Larrasoaña et al., 2003). In these studies, meridional shifts in the Hadley cell and the tropics are associated to changes in the equator-to-pole insolation gradient, which in summer has a strong obliquity component. These studies also suggest that the insolation gradient over the austral winter hemisphere causes temperature and trade wind changes that can influence the intensity and poleward penetration of the boreal summer monsoons. However, the winter (intrahemispheric) insolation gradient does not vary with obliquity, but with precession (Davis and Brewer, 2009), so changes in winter hemisphere insolation gradients cannot be used to explain (low-latitude) obliquity signals. Also, we suggest that while the Hadley cell, and thus precipitation patterns, might indeed shift on obliquity time scales due to changes the (summer) equator-to-pole gradient, such a shift does not explain the changes in precipitation amounts, the strength of the Hadley circulation and the strength of cross-equatorial winds and moisture transport that we identify in our obliquity experiments. Further sensitivity studies could shed more light on the relative roles of inter- and intra-hemispheric gradients (see Sect. 4.3).

4.2 Implications for the interpretation of paleoclimate records

Obliquity signals in low-latitude paleoclimate records are often interpreted using the 65° N 21 June insolation curve based on the matching precession-obliquity interference in the records and the 65° N insolation curve. The model study of Tuenter et al. (2003), indicating that ~ 80–90 % of the obliquity signal in the North-African monsoon is due to high latitude influences, supported the use of the 65° N insolation curve. Some studies, on the other hand, used a P-$\frac{1}{2}$T curve to interpret paleoclimate records (e.g. Lourens et al., 1996). This combination of the precession and obliquity parameters is very similar to the 65° N 21 June insolation curve, but by using P-$\frac{1}{2}$T no direct assumptions on climate mechanisms are made. Our results, based on a much more sophisticated (and realistic) model with fixed land ice, clearly suggest a low-latitude mechanism for obliquity patterns at low latitudes through a direct response to changes in the cross-equatorial insolation gradient. Furthermore, there is a strong resemblance between (boreal) SITIG and the 65° N 21 June insolation curve (Fig. 6, Lourens and Reichart, 1996; Leuschner and Sirocko, 2003) as well as the P-$\frac{1}{2}$T curve (Lourens et al., 2001). Hence, the widely applied 65° N 21 June insolation curve (Tiedemann et al., 1994; Hilgen et al., 1995, 2000; Lourens et al., 1996, 2001; Sierro et al., 2000) needs to be reconsidered in favour of SITIG. SITIG instead of 65° N 21 June insolation relies on a physical basis as described by our model results rather than pattern matching, and

CPD
11, 221–241, 2015

explains the obliquity influence on tropical climate independently of glacial-interglacial variability.

We note that the original SITIG theory was based on the Mediterranean sapropels (Lourens and Reichart, 1996), which were originally linked to North African monsoon strength (e.g. Rossignol-Strick, 1985; Ruddiman, 2007), but have recently also been attributed to changes in Mediterranean winter precipitation through changes in Atlantic storm track activity (e.g. Tzedakis, 2007; Brayshaw et al., 2011; Kutzbach et al., 2013). In our obliquity experiments, changes in winter precipitation are unrelated to the Atlantic storm tracks, but are of equal magnitude as monsoonal runoff into the Mediterranean. In terms of percentages, however, changes in monsoonal runoff are larger (Bosmans et al., 2014b). Another study stating the importance of cross-equatorial insolation gradients, (Leuschner and Sirocko, 2003), is based the insolation difference between 30° N and 30° S, which drives Indian summer monsoon strength through pressure differences. Leuschner and Sirocko (2003) state that their record of continental dust transport (indicative of monsoon strength) responds immediately to changes in the cross-equatorial insolation gradient. This matches with our results, showing changes in Indian summer monsoon strength as well as cross-equatorial winds and moisture transport that are particularly strong over the Indian Ocean. Also, other paleoclimate records in the Arabian Sea have been used to rule out global ice volume as a primary forcing mechanism for the occurrence of obliquity-related variability in the Indian monsoon (Clemens et al., 1991; Clemens and Prell, 2003). Therefore we conclude that, despite the need to determine the relative role of (winter) precipitation over the Mediterranean in the formation of the sapropels, there is sufficient evidence from tropical and sub-tropical paleoclimate records suggesting a local, direct response to obliquity forcing.

4.3 Obliquity-induced gradients and their influence on global climate

Lourens and Reichart (1996) and Leuschner and Sirocko (2003) suggested that through monsoon-induced changes in atmospheric moisture content, a strong greenhouse gas, the Summer Inter Tropical Insolation Gradient (SITIG) may drive glacial-interglacial variability. Indeed we find a significant obliquity-induced change in cross-equatorial moisture transport (Figs. 2b and d). However, whether changes in atmospheric moisture content resulting from changes in low-latitude atmospheric circulation on orbital time scales can indeed result in global climate change will need to be investigated with longer model experiments including dynamic ice sheets (not included in EC-Earth). Furthermore, despite having a relatively strong obliquity component, the precession component in SITIG is stronger (Fig. 6). Precession, however, has an opposite effect on both hemispheres. Moisture changes during boreal summer may therefore be exactly opposite to moisture changes during austral summer, so the precession signal in atmospheric moisture content is canceled out. Lourens and Reichart (1996) suggest that in this case SITIG can account for the obliquity-dominated glacial variability between ~ 2.7 and 1 million years ago. Given the larger landmasses, and hence stronger monsoons, on the Northern Hemisphere we do not think that the precession effect cancels out, so SITIG will not result in a purely obliquity-paced signal in moisture content.

Another mechanism by which obliquity can affect high-latitude climate and glacial cycles through latitudinal insolation gradients has been proposed by Raymo and Nisancioglu (2003); Vettoretti and Peltier (2004); Antico et al. (2010); Mantsis (2011). These studies suggest that the poleward transport of heat, moisture and latent energy is increased during minimum obliquity due to the intensified intrahemispheric (equator-to-pole) insolation and temperature gradient. The increased moisture transport towards the poles combined with low polar temperatures during low obliquity is favourable for ice growth. In our EC-Earth experiments we also find stronger poleward moisture transport outside the tropics during minimum obliquity (Tmin) during both boreal and austral summer as well as in the annual mean (not shown). Furthermore, changes in poleward energy transport by ocean currents can play a role in obliquity's effect on global climate (Khodri et al., 2001; Jochum et al., 2012). In order to determine the relative role of tropical circulation changes through interhemispheric insolation gradients (SITIG), compared to changes in poleward energy and moisture transport in both atmosphere and ocean through intrahemispheric gradients, further sensitivity experiments are necessary. Such experiments should include dynamic ice sheets and should be run longer for ice sheets and the (deep) ocean to equilibrate to the obliquity forcing. At this point such experiments are not yet feasible with the EC-Earth model.

5 Conclusions

The low-latitude SITIG mechanism proposed here is fundamentally different from high-latitude mechanisms previously proposed to explain the obliquity patterns at low latitudes. Our results, based on the sophisticated model EC-Earth, suggest that these patterns arise from a direct response to changes in the cross-equatorial insolation gradient, i.e. without any influence of ice sheets or other high-latitude mechanisms. Hence, the widely applied 65° N 21 June insolation curve needs to be reconsidered in favour of SITIG.

Acknowledgements. The EC-Earth experiments were performed at KNMI using ECMWF facilities. This work was part of Joyce Bosmans' Ph.D. project, funded by a "Focus en Massa" grant at Utrecht University.

References

Antico, A., Marchal, O., Mysak, L., and Vimeux, F.: Milankovitch forcing and meridional moisture flux in the atmosphere: insight from a zonally averaged ocean–atmosphere model, J. Climate, 23, 4841–4855, 2010. 224, 231

Bloemendal, J. and deMenocal, P.: Evidence for a change in the periodicity of tropical climate cycles at 2.4 Myr from whole-core magnetic susceptibility measurements, Nature, 342, 897–900, 1989. 223

Bosmans, J. H. C., Drijfhout, S. S., Tuenter, E., Lourens, L. J., Hilgen, F. J., and Weber, S. L.: Monsoonal response to mid-holocene orbital forcing in a high resolution GCM, Clim. Past, 8, 723–740, doi:10.5194/cp-8-723-2012, 2012. 225

Bosmans, J. H. C., Drijfhout, S. S., Tuenter, E., Hilgen, F. J., and Lourens, L. J.: Response of the North African summer monsoon to precession and obliquity forcings in the EC-Earth GCM, Clim. Dynam., 44, 279–297, doi:10.1007/s00382-014-2260-z, 2014a. 222, 224, 226

Bosmans, J. H. C., Drijfhout, S. S., Tuenter, E., Hilgen, F. J., Lourens, L. J., and Rohling, E. J.: Precession and obliquity forcing of the freshwater budget over the Mediterranean, Quaternary Sci. Rev., in review, 2014b. 230

Brayshaw, D. J., Rambeau, C. M. C., and Smith, S. J.: Changes in Mediterranean climate during the Holocene: insight from global and regional climate modelling, Holocene, 21, 15–31, doi:10.1177/0959683610377528, 2011. 230

Clemens, S. C. and Prell, W. L.: A 350 000 year summer-monsoon multi-proxy stack from the Owen Ridge, Northern Arabian Sea, Mar. Geol., 201, 35–51, 2003. 223, 230

Clemens, S., Prell, W., Murray, D., Shimmield, G., and Weedon, G.: Forcing mechanisms of the Indian Ocean monsoon, Nature, 353, 720–725, 1991. 223, 230

Davis, B. A. S. and Brewer, S.: Orbital forcing and the role of the latitudinal insolation/temperature gradient, Clim. Dynam., 32, 143–165, doi:10.1007/s00382-008-0480-9, 2009. 229

deMenocal, P. B.: Plio-Pleistocene African climate, Science, 270, 53–59, 1995. 223

deMenocal, P. B., Ruddiman, W. F., and Pokras, E. M.: Influences of high- and low-latitude processes on African terrestrial climate: Pleistocene eolian records from equatorial Atlantic ocean drilling program site 663, Paleoceanography, 8, 209–242, 1993. 223

Hazeleger, W., Wang, X., Severijns, C., Stefanescu, S., Bintanja, R., Sterl, A., Wyser, K., Semmler, T., Yang, S., van den Hurk, B., van Noije, T., van der Linden, E., and van der Wiel, K.: EC-Earth V2.2: description and validation of a new seamless earth system prediction model, Clim. Dynam., 39, 2611–2629, doi:10.1007/s00382-011-1228-5, 2011. 225

Hilgen, F., Krijgsman, W., Langereis, C., Lourens, L., Santarelli, A., and Zachariasse, W.: Extending the astronomical (polarity) time scale into the Miocene, Earth Planet. Sc. Lett., 136, 495–510, 1995. 223, 229

Hilgen, F. J., Bissoli, L., Iaccarino, S., Krijgsman, W., Meijer, R., Negri, A., and Villa, G.: Integrated stratigraphy and astrochronology of the Messinian GSSP at Oued Akrech (Atlantic Morocco), Earth Planet. Sc. Lett., 182, 237–251, 2000. 223, 229

Jochum, M., Jahn, A., Peacock, S., Bailey, D. A., Fasullo, J. T., Kay, J., Levis, S., and Otto-Bliesner, B.: True to Milankovitch: glacial inception in the New Community Climate System Model, J. Climate, 25, 2226–2239, doi:10.1175/JCLI-D-11-00044.1, 2012. 231

Khodri, M., Leclainche, Y., Ramstein, G., Braconnot, P., Marti, O., and Cortijo, E.: Simulating the amplification of orbital forcing by ocean feedbacks in the last glaciation, Nature, 410, 570–574, 2001. 231

Kutzbach, J. E., Chen, G., Cheng, H., Edwards, R., and Liu, Z.: Potential role of winter rainfall in explaining increased moisture in the Mediterranean and Middle East during periods of maximum orbitally-forced insolation seasonality, Clim. Dynam., 42, 1079–1095, doi:10.1007/s00382-013-1692-1, 2013. 230

Larrasoaña, J. C., Roberts, A. P., Rohling, E. J., Winklhofer, M., and Wehausen, R.: Three million years of monsoon variability over the northern Sahara, Clim. Dynam., 21, 689–698, doi:10.1007/s00382-003-0355-z, 2003. 228

Leuschner, D. C. and Sirocko, F.: Orbital insolation forcing of the Indian monsoon – a motor for global climate changes?, Palaeogeogr. Palaeocl., 197, 83–95, 2003. 224, 228, 229, 230

Lin, J. L.: The double-ITCZ problem in IPCC AR4 coupled GCMs: ocean–atmosphere feedback analysis, J. Climate, 20, 4497–4525, 2007. 227

Lourens, L. and Reichart, G.-J.: Low latitude forcing of glacial cycles, in: Late Quaternary Variability of the Arabian Sea Monsoon and Oxygen Minimum Zone, Ph. D. thesis, Utrecht University, 153–168, 1996. 222, 224, 228, 229, 230, 231

Lourens, L. J., Antonarakou, A., Hilgen, F. J., Hoof, A. A. M. V., and Zachariasse, W. J.: Evaluation of the Plio-Pleistocene astronomical timescale, Paleoceanography, 11, 391–413, 1996. 222, 223, 229

Lourens, L. J., Wehausen, R., and Brumsack, H. J.: Geological constraints on tidal dissipation and dynamical ellipticity of the Earth over the past three million years, Nature, 409, 1029–1034, 2001. 223, 229

Lourens, L., Becker, J., Bintanja, R., Hilgen, F., Tuenter, E., van de Wal, R., and Ziegler, M.: Linear and non-linear response of late Neogene glacial cycles to obliquity forcing and implications for the Milankovitch theory, Quaternary Sci. Rev., 29, 352–365, 2010. 223

Mantsis, D. F.: Atmospheric response to orbital forcing and 20th century sea surface temperatures, Ph. D. thesis, University of Miami, available at: http://scholarlyrepository.miami.edu/oa_dissertations/597, 2011. 224, 231

Opsteegh, J., Haarsma, R., Selten, F., and Kattenberg, A.: ECBILT: a dynamic alternative to mixed boundary conditions in ocean models, Tellus A, 50, 348–367, 1998. 224

Raymo, M. E. and Nisancioglu, K.: The 41 kyr world: Milankovitch's other unsolved mystery, Paleoceanography, 18, doi:10.1029/2002PA000791, 2003. 224, 231

Rossignol-Strick, M.: Mediterranean Quaternary sapropels, an immediate response of the African monsoon to variation of insolation, Palaeogeogr. Palaeocl., 49, 237–263, 1985. 223, 228, 230

Ruddiman, W. F.: Earth's Climate: Past and Future, W. H. Freeman, available at: http://books.google.nl/books?id=Mpj_GwAACAAJ, 2007. 230

Sierro, F., Ledesma, S., Flores, J., Torrescusa, S., and Martinez del Olmo, W.: Sonic and gamma-ray astrochronology: cycle to cycle calibration of Atlantic climatic records to Mediterranean sapropels and astronomical oscillations, Geology, 28, 695–698, 2000. 223, 229

Tiedemann, R., Sarnthein, M., and Shackleton, N. J.: Astronomic timescale for the Pliocene Atlantic δ^{18}O and dust flux records of Ocean Drilling Program Site 659, Paleoceanography, 9, 619–638, 1994. 223, 229

Tuenter, E., Weber, S. L., Hilgen, F. J., and Lourens, L. J.: The response of the African summer monsoon to remote and local forcing due to precession and obliquity, Global Planet. Change, 36, 219–235, doi:10.1016/S0921-8181(02)00196-0, 2003. 222, 224

Tzedakis, P. C.: Seven ambiguities in the Mediterranean palaeoenvironmental narrative, Quaternary Sci. Rev., 26, 2042–2066, 2007. 230

Vettoretti, G. and Peltier, W.: Sensitivity of glacial inception to orbital and greenhouse gas climate forcing, Quaternary Sci. Rev., 23, 499–519, 2004. 231

CPD

11, 221–241, 2015

Obliquity forcing of low-latitude climate

J. H. C. Bosmans et al.

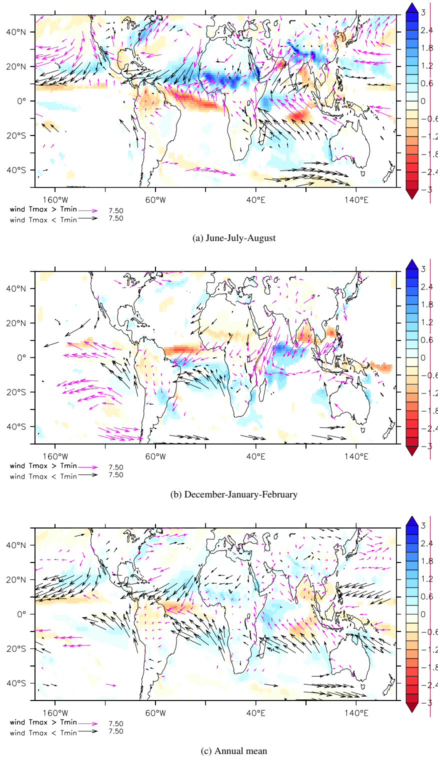

Figure 1. Net precipitation differences and *T*max surface wind for JJA **(a)**, DJF **(b)** and annual mean **(c)**. For net precipitation (precipitation minus evaporation), the differences (*T*max minus *T*min) are shown in mm day^{-1}. Overlain are the wind vectors for *T*max in m s^{-1}. Purple vectors indicate larger windspeeds during *T*max than during *T*min. Cross-equatorial winds are stronger in JJA **(a)** and DJF **(b)**, mostly over the Atlantic and Indian Ocean. Every 7th arrow in the *x* direction is drawn and every 4th arrow in the *y* direction. Results are only shown where the differences in net precipitation or windspeeds are statistically significant at 95 % (based on a two-sided Student *t* test). The full wind field is given in Fig. 3.

CPD
11, 221–241, 2015

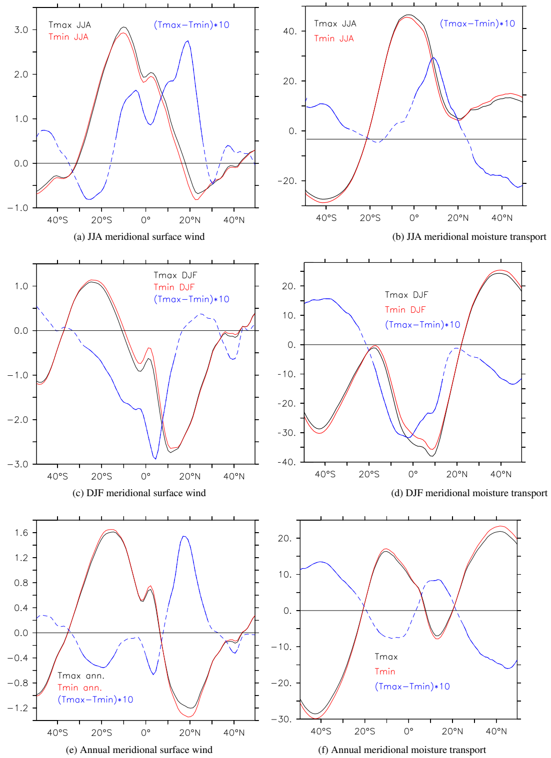

Figure 2. Zonal mean meridional surface wind and moisture transport for JJA **(a, b)**, DJF **(c, d)** and annual mean **(e, f)**. The wind is given in $\mathrm{m\,s^{-1}}$, moisture transport in $\mathrm{kg\,(ms)^{-1}}$ for both Tmax (black), Tmin (red) and the difference (blue, multiplied by 10 for clarity). Moisture transport is calculated as the mass-weighted vertical integral of specific humidity multiplied by horizontal wind. Positive values indicate northward wind or moisture transport, negative values southward. Wind and moisture transport into the summer hemisphere is stronger during Tmax for JJA **(a, b)** and DJF **(c, d)**. Solid parts of the blue line indicate where the difference is statistically significant at 95 % (based on a two-sided Student t test). Note that the vertical scales are different.

CPD
11, 221–241, 2015

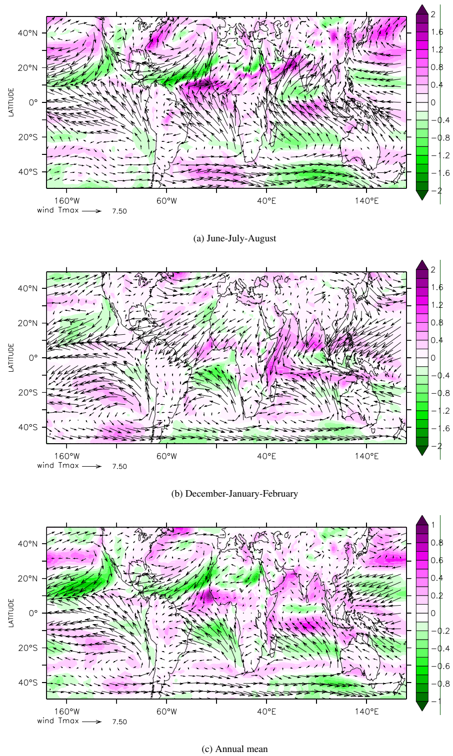

Figure 3. Wind during Tmax in JJA **(a)**, DJF **(b)** and the annual mean **(c)**, in m s^{-1}. The colour scale indicates the difference in windspeed between Tmax and Tmin, in m s^{-1}. Note the different colour scale for the annual mean. Every 9th vector is shown in the x direction, and every 5th in the y direction.

CPD
11, 221–241, 2015

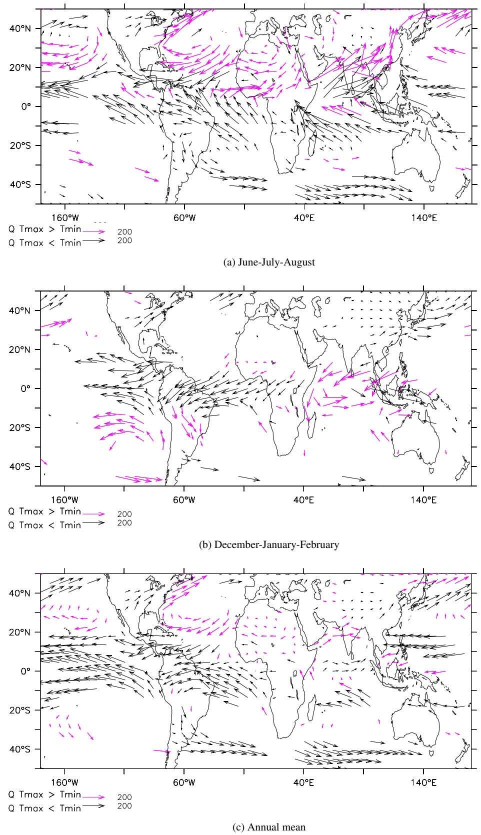

Figure 4. Moisture transport in Tmax for JJA **(a)**, DJF **(b)** and annual mean **(c)**, vertically integrated, in kg(ms)$^{-1}$. Purple vectors indicate larger moisture transport during Tmax than during Tmin. Every 7th arrow in the x direction is drawn and every 4th arrow in the y direction. Results are only shown where the differences are statistically significant at 95 % (based on a two-sided Student t test).

CPD
11, 221–241, 2015

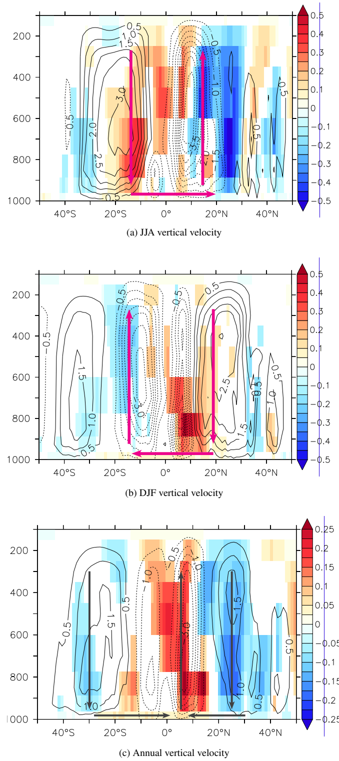

Figure 5. Zonal mean vertical velocity (omega, 10^{-2} Pa s^{-1}) during Tmax (contours) for JJA **(a)**, DJF **(b)** and annual mean **(c)**. Negative contours indicate upward motion (rising), positive contours indicate downward motion (sinking). The vertical scale (y axis) denotes height in hPa. The colours indicate the differences between Tmax and Tmin, only shown where they are statistically significant at 95 % (based on a two-sided Student t test). The arrows indicate the direction of the air flow and are purple where the flow is stronger during Tmax compared to Tmin, which is the case for boreal and austral summer **(a, b)**. Black arrows indicate where the flow is weaker during Tmax. Note the different colour scale for the annual mean.

CPD
11, 221–241, 2015

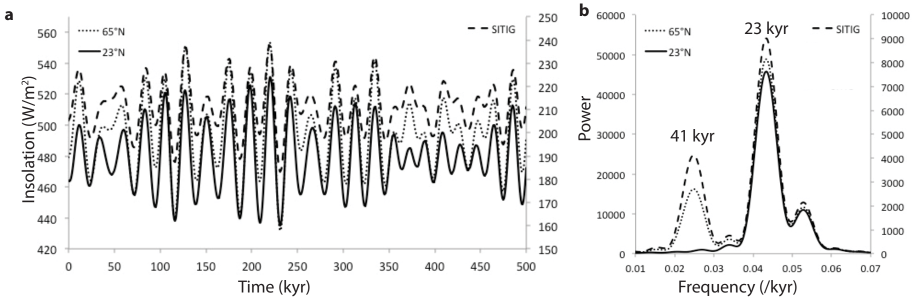

Figure 6. Insolation over the past 500 kyr **(a)** at 23° N (solid line) and 65° N (dotted line) on the left *y* axis and SITIG (insolation difference between 23° N and 23° S at 21 June, dashed line) on the right *y* axis. **(b)** shows the power spectra of these three insolation curves, with peaks at 23 kyr (precession) and 41 kyr (obliquity), again the left *y* axis is for 23° N and 65° N insolation, the right *y* axis for SITIG.

CPD
11, 221–241, 2015